Full Paper
doi.org/10.1002/chem.202101921

Chemistry Europe
European Chemical Societies Publishing

Atypical and Asymmetric 1,3-P,N Ligands: Synthesis, Coordination and Catalytic Performance of Cycloiminophosphanes

Mark K. Rong,[a] Flip Holtrop,[a] Eduard O. Bobylev,[a] Martin Nieger,[b] Andreas W. Ehlers,[a, c, d] J. Chris Slootweg,[a, d] and Koop Lammertsma*[a, c]

Abstract: Novel seven-membered cyclic imine-based 1,3-P,N ligands were obtained by capturing a Beckmann nitrilium ion intermediate generated in situ from cyclohexanone with benzotriazole, and then displacing it by a secondary phosphane under triflic acid promotion. These "cycloiminophosphanes" possess flexible non-isomerizable tetrahydroazepine rings with a high basicity; this sets them apart from previously reported iminophophanes. The donor strength of the ligands was investigated by using their P-κ^1- and P,N-κ^2-tungsten(0) carbonyl complexes, by determining the IR frequency of the *trans*-CO ligands. Complexes with $[RhCp^*Cl_2]_2$ demonstrated the hemilability of the ligands, giving a dynamic equilibrium of κ^1 and κ^2 species; treatment with AgOTf gives full conversion to the κ^2 complex. The potential for catalysis was shown in the Ru^{II}-catalyzed, solvent-free hydration of benzonitrile and the Ru^{II}- and Ir^{I}-catalyzed transfer hydrogenation of cyclohexanone in isopropanol. Finally, to enable access to asymmetric catalysts, chiral cycloiminophosphanes were prepared from L-menthone, as well as their P,N-κ^2-Rh^{III} and a P-κ^1-Ru^{II} complexes.

Introduction

Ligand-based reactivity can enhance the activity of transition metal catalysts,[1] as is the case for hybrid ligands,[2] which combine the properties of different heteroatoms to enable hemilability, redox non-innocence, proton shuttling, and substrate coordination.[1,2] 1,3-P,N ligands are particularly subject to diverse binding modes (N-κ^1, P-κ^1, P-$\kappa^1\eta^2$, κ^2, and μ; Figure 1) and their complexes have found application in homo/heterogeneous catalysis, bio-inorganic chemistry, and photoluminescence.[3–7] Most of these 1,3-P,N complexes are based on pyridyl- and imidazolyl-based ligands **A** and **B**, which have structural limitations that are inherent to their syntheses.[4c,5a,b] Recently we reported on the highly tunable iminophosphanes **C** and their tautomers phosphaamidines **D** that can be independently substituted on the P, C, and N atoms.[6,7] These 1,3-P,N ligands are readily accessible from (base-stabilized) nitrilium triflate precursors and even though they are obtained as (dynamic) *E*/*Z* isomer mixtures, the equilibrium shifts to the desired *Z* conformer on coordination to metals (Figure 2).[6] The hapticity in κ^1/κ^2-[(P,N)RhCp*Cl$_2$]-complexes and the favorable performance in (κ^1-P,N)-Ru^{II}-catalyzed nitrile hydration correlated with the electronic properties of the ligands[6d] and the basicity of the nitrogen donor (Figure 3).[3,4]

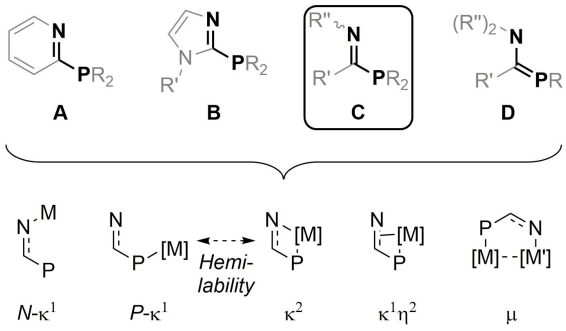

Figure 1. 1,3-P,N ligands and their diverse transition metal complexes.

Iminophosphanes **C** are accessed from nitrilium ion precursors, which are known both as reactive synthons and intermediates.[5,8] Illustrative is the Beckmann rearrangement of cyclohexanone oxime to the ring-expanded seven-membered

[a] M. K. Rong, F. Holtrop, E. O. Bobylev, Dr. A. W. Ehlers, Dr. J. C. Slootweg, Prof. Dr. K. Lammertsma
Department of Chemistry and Pharmaceutical Sciences
Vrije Universiteit Amsterdam
De Boelelaan 1083, 1081 HV Amsterdam (The Netherlands)
E-mail: k.lammertsma@vu.nl

[b] Dr. M. Nieger
Department of Chemistry, University of Helsinki
A. I. Virtasen aukio 1, P.O. Box 55, FIN-00014Helsinki (Finland)

[c] Dr. A. W. Ehlers, Prof. Dr. K. Lammertsma
Department of Chemistry, University of Johannesburg
Oakland Park, 2006, Johannesburg (South Africa)

[d] Dr. A. W. Ehlers, Dr. J. C. Slootweg
Present address: Van 't Hoff Institute for Molecular Sciences
University of Amsterdam
P.O. Box 94157, 1090 GD Amsterdam (The Netherlands)

Supporting information for this article is available on the WWW under https://doi.org/10.1002/chem.202101921

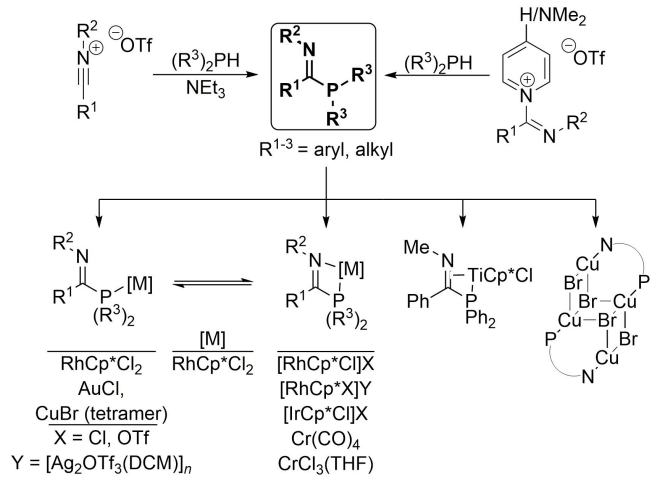

Figure 2. Synthesis of iminophosphanes and hemilabile metal coordination.

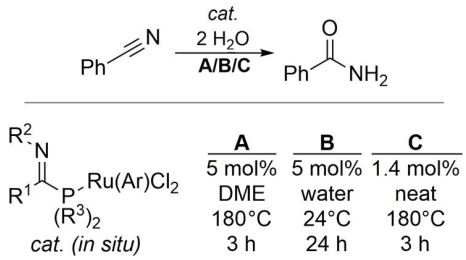

Figure 3. Catalyzed nitrile hydration.

nitrilium intermediate (with an iminium resonance form), which hydrolyzes to the ε-caprolactam that is used as the building block for the commercial production of nylon-6 (Figure 4, top).[9,10] The intermediate can also be trapped by nucleophiles, for instance by benzotriazole,[11] which under Lewis acid promotion can be displaced by other nucleophiles.[11a] This reactivity mirrors our reported nitrilium triflate approach for the synthesis of **C** and might be suitable to access novel 7-membered cyclic iminophosphanes (Figure 4**E**). Such "cyclo-iminophosphanes" would be conformationally locked, that is, unable to undergo *E*/*Z* isomerization, which could boost their

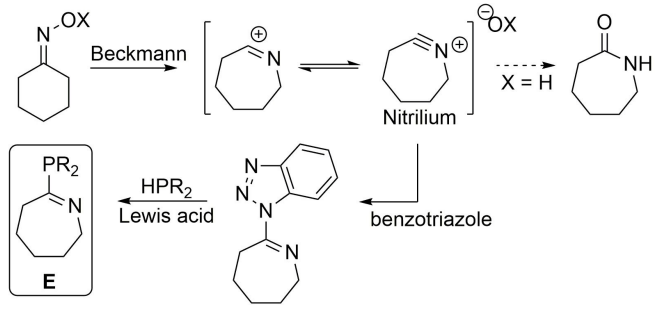

Figure 4. Cycloiminophosphane synthesis from the Beckmann nitrilium intermediate.

efficiency (Figure 5). Moreover, the ring might carry chiral groups as the required chiral cyclohexanone precursors are readily available from terpenoids used in, for instance, the flavoring and perfume industry.[12]

In this study, we report both the synthesis of these novel cyclic 1,3-P,N ligands and their surprising electronic properties that set them apart from noncyclic iminophosphanes. We explore their coordination to early and late transition metals in κ^1/κ^2 complexes and assess their performance in catalytic nitrile hydration and transfer hydrogenation. Crystal structures are provided for the (a)symmetric tetrahydroazepine synthons, ligands, and a W complex.

Results and Discussion

The synthesis of the cyclic ligands is discussed first, followed by an analysis of their donor capacity using IR- and ^{31}P NMR spectroscopy on W^0 carbonyl complexes and dynamic Rh^{III} complexes, respectively. Next, Ru^{II} species are examined to evaluate the ligands' performance in homogeneous catalysis. We also discuss analogous asymmetric ligands with a natural product-derived backbone.

Precursor synthesis

Our synthetic strategy is based on reacting phosphanes with a seven-membered ring nitrilium ion, that is, the 3,4,5,6-tetrahydro-azepinium ion.[10] Because this ion could not be accessed by our established methodology in which amides are reacted to imidoyl halides with subsequent halide to triflate exchange,[6] as the activating agents converted ε-caprolactam to thick intractable mixtures of presumably protonated imidoyl chloride, dimers and/or nylon like polymers,[13,14] we decided to generate the desired nitrilium ion in situ using the Beckmann rearrangement and trap it with benzotriazole.[11]

Treating neat cyclohexanone with hydroxylamine·HCl salt by grinding them together in a mortar, while slowly adding NaOH, yielded the corresponding pure oxime conveniently, even on large scale (120 mmol, 82%; Scheme 1).[15] Next, under an atmosphere of nitrogen, the oxime was activated in situ as the corresponding methylsulfonate with methylsulfonyl chloride and triethylamine in MeCN at 0 °C.[11c,16] Benzotriazole was added and the mixture was heated to reflux for 2 h to facilitate the ring expansion and trap the nitrilium ion. The reported work-up[11c] was significantly simplified by adding

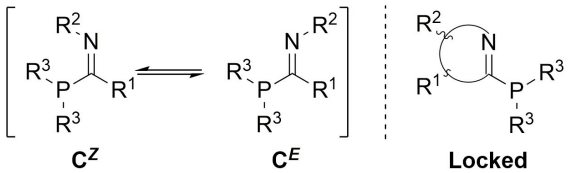

Figure 5. Non-isomerizable cycloiminophosphanes.

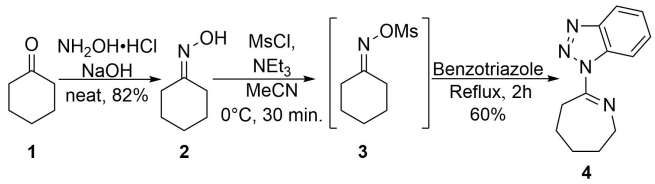

Scheme 1. Synthesis of benzotriazolyl-tetrahydroazepine.

water to the crude mixture to precipitate pure **4** as a white solid in good yield (60%); alternatively, evaporation, extraction into Et_2O and filtration over neutral alumina also provides **4** (58%). Single crystals suitable for X-ray diffraction analysis were obtained from Et_2O and revealed a remarkably flat conformation [N1–C1–N2–N3 = 179.54(8); C6–C1–N2–N3 = −0.37(12)],

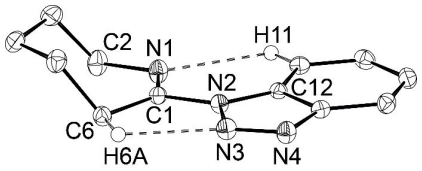

Figure 6. Displacement ellipsoid plot of benzotriazolyl tetrahydroazepine **4** at the 50% probability level. Hydrogen atoms are omitted for clarity, with the exception of H6A and H11. Selected bond lengths [Å] and angles [°]: C1–N1 = 1.2643(13), C1–N2 = 1.4334(12), N1–C2 = 1.4693(12), C1–C6 = 1.5046(13), N2–N3 = 1.3746(11), N3–N4 = 1.2947(12), N2–C12 = 1.3780(12), N3···H6A = 2.29, N1···H11 = 2.50, N1–C1–N2 = 114.81(9), N1–C1–C6 = 129.01(9), N2–C1–C6 = 116.18(8), C1–N1–C2 = 118.88(9), N1–C1–N2–N3 = 179.54(8), C6–C1–N2–N3 = −0.37(12).

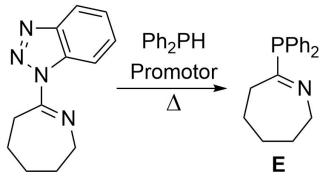

Scheme 2. The activation of **4** for Ph_2PH introduction.

Table 1. Lewis acid induced exchange of the benzotriazolyl group of **4** for PPh_2.[a]

	Promotor	Loading [mol%]	Solvent	*t* [min.]	Conversion to **E** [%]	Selectivity for **E** [%][b]
1[c]	$AlCl_3$	10%	$CHCl_3$	10	25	100
2	$AlCl_3$	10%	$CHCl_3$	90	40	95
3	$AlCl_3$	10%	$CHCl_3$	300	57	88
4	$AlCl_3$	25%	$CHCl_3$	90	64	93
5	$AlCl_3$	100%	$CHCl_3$	90	99	99[d]
6	$SnCl_2$	100%	$CHCl_3$	90	70	95
7	$SnCl_2$	100%	$CHCl_3$	300	72	97
8	$SnCl_2$	100%	Toluene	300	36	63
9	$SnCl_4$	100%	$CHCl_3$	300	50	50
10	BF_3OEt_2	100%	$CHCl_3$	300	76	92
11[e]	HOTf	100%	$CHCl_3$	10	100	100

[a] Conditions: 1 equiv. Ph_2PH, solvent (0.35 M), reflux. [b] Determined by ^{31}P NMR spectroscopy. [c] $T = 80\,^{\circ}C$, μW conditions, 0.25 M. [d] Conversion to the $AlCl_3$ adduct of **6**. [e] RT, 0.5 M.

presumably due to N1···H11 and N3···H6A hydrogen bonding (2.50 and 2.29 Å, respectively; Figure 6). The C1–N1 bond length of 1.2643(13) Å is typical for an imine bond and the C1–N2 bond of 1.4334(12) Å is similar to those of other N-heterocycle-stabilized imines.[6c]

Phosphane introduction

In analogy to the formation of **4**, we tried to capture the in situ generated 3,4,5,6-tetrahydro-azepinium ion directly with a phosphane to obtain the desired cycloiminophosphane ligand **E**, but to no avail. Instead, the benzotriazole group of **4** could be replaced for diphenylphosphane using Lewis acid promotion, which we examined under a variety of conditions (Scheme 2, Table 1). We started with a microwave reaction employed in related displacements by N nucleophiles,[11a] but this reaction using 10 mol% $AlCl_3$ (entry 1) proved to be less effective than regular heating under reflux (entries 2 and 3). The still modest conversion, probably due to Lewis pair interaction with the phosphane,[17] could be enhanced by increasing the amount of $AlCl_3$ (entries 4 and 5). Using equimolar amounts, $AlCl_3$ proved to be more selective than $SnCl_2$, $SnCl_4$, and BF_3 (entries 5–10) and resulted in 99% conversion to an Al adduct of the desired ligand, which on treatment with water gave the protonated ligand and a mixture of oxy aluminum anions. However, the by far most effective and convenient manner to obtain the protonated ligand was found to be the direct activation of **4** through protonation with triflic acid (entry 11).

Treatment of **4** with 1 equiv. of triflic acid at 0 °C resulted instantly in a suspension from which its iminium form **5** could be isolated by filtration (Scheme 3). Whereas **5** is subject to decomposition over time, both in solution and as an isolated solid, it reacted cleanly upon immediate resuspension with phosphanes to give **6** within minutes. After work-up, diphenyl derivative **6a** was obtained in 77% as an air-stable solid. The aliphatic derivatives **6b** and **6c** (conversion 85% (*n*Bu) and 66% (Cy)) could not be purified satisfactorily until after the subsequent deprotonation step (see below). Bulky substituents may hinder the formation of **6**, as suggested by the lower selectivity found for **6c**. Crystals suitable for X-ray diffraction could be obtained for **6a** and **6c** by slow diffusion of pentane into a THF solution. The molecular structures show a chair conformation for the tetrahydroazepine rings, with the P-lone pair facing away from the imine (Figure 7). Generally, the structures are comparable to those reported for noncyclic

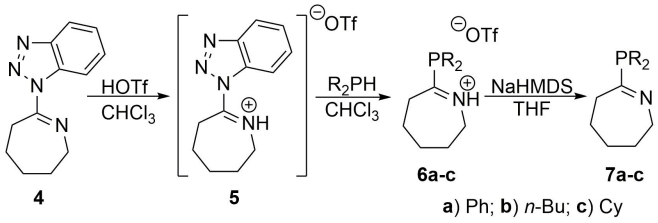

Scheme 3. Acid-facilitated activation of **4** to give ligands **6** and **7**.

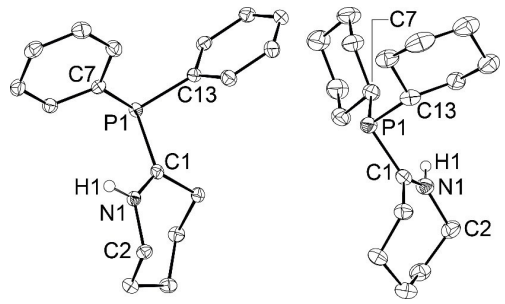

Figure 7. Displacement ellipsoid plot of phosphaazepinium triflates **6a** (left) and **6c** (right) at the 50% probability level. C–H hydrogen atoms and the triflate anions are omitted for clarity. Selected bond lengths [Å] and angles [°] of **6a**: P1–C1 = 1.8269(13), P1–C7 = 1.8249(13), P1–C13 = 1.8223(13), C1–N1 = 1.2858(16), N1–C2 = 1.4839(16), N1–H1 = 0.869(13), N1–C1–P1 = 123.06(10) N1–C1–C6 = 119.70(11), C1–N1–C2 = 125.03(11); Selected bond lengths (Å) and angles (°) of **6c**: P1–C1 = 1.8310(16), P1–C7 = 1.8478(15), P1–C13 = 1.8697(16), C1–N1 = 1.2892(19), N1–C2 = 1.4779(19), N1–C1–P1 = 124.44(12), N1–C1–C6 = 120.25(14), C1–N1–C2 = 125.72(13).

iminophosphane ligands.[6a,b] The imine bond lengths are in the expected range [**6a**: N1–C1 = 1.2858(16) Å; **6c**: N1–C1 = 1.2892(19) Å], as are the P–C bonds [**6a**: P1–C1 = 1.8269(13) Å; **6c**: P1–C1 = 1.8310(16) Å].[18]

Compounds **6a–c** could be readily deprotonated in THF by using NaHMDS as base at −78 °C and then extracted into pentane to provide the desired novel ligands (**7a**: 92%; **7b**: 83%; **7c**: 76% yield). Surprisingly, and in contrast to **6**, the products show sets of two distinct ^{31}P NMR signals [**7a**: δ 6.0 (14%), 5.4 (86%); **7b**: δ −10.7 (95%), −17.5 (5%); **7c**: δ 17.5 (88%), 13.5 (12%)]. Conformational flips of the aliphatic rings, known as flippamers, are known to be observable by NMR spectroscopy,[19] and this may also be the case for the tetrahydroazepine ring in **7** (Figure 8, with the presumed major conformer in the center).

A striking property of **7** is its relative basicity. For example, dissolving **7** in $CDCl_3$ led to its instant decomposition, presumably due to protonation (chloroform pK_a > 16). Compared to known iminophosphanes, the seemingly higher basicity of **7** could be attributed to its C- and N-alkyl

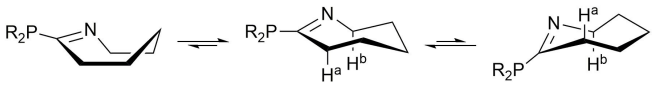

Figure 8. Possible tetrahydroazepine-ring conformations (flippamers) for **7a–c**. Two axial protons are marked for clarity.

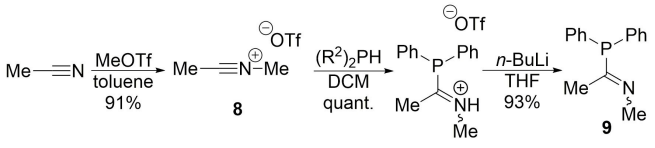

Scheme 4. Synthesis of **8**, the noncyclic analogue of **7a**.

substituents. For comparison, we synthesized noncyclic C,N-dimethyl iminophosphane **9** from the nitrilium ion obtained by methylation of acetonitrile (**8**, 91%)[20] and diphenylphosphane (Scheme 4). Also in this case, a strong base (*n*BuLi) was needed to generate the 1,3-P,N product (93%; δ(^{31}P) = 6.7 (*E*), −13.2 (*Z*)), whereas NEt_3 (p$K_a \approx 11$) sufficed for previously reported ligands.[6] The unexpected high basicity of **7** seems akin to that of structurally related 1,3-N,N bases such as DBU.[21]

Coordination chemistry and catalysis

The donor strength of P,N ligands affects their efficiency in cooperative reactions.[3,4,6] To examine the influence of **7** in transition metal complexes, we synthesized the tungsten carbonyl complexes **10** and **11** as the IR frequency of their *trans*-CO ligands reflect the ligand's P,N donor strength.[22] Treating ligand **7a** with either [$W(CO)_5$(MeCN)] or [(COD)$W(CO)_4$] provided, respectively, κ^1-complex **10** (82%) and κ^2-complex **11** (83%; Scheme 5). IR spectroscopic analysis of the *trans*-CO ligands indicated increasing electron donation to the metal for **11** (2069, 2008 (*trans*), 1869, 1825 cm^{-1}) with respect to **10** (2069 (*trans*), 1904, 1873 cm^{-1}). Compared to the analogous W complexes of the widely applied Ph_2PPy ligand (Figure 1, **A**; κ^1: 2050, 1980, 1920 cm^{-1}; κ^2: 2017, 1890, 1870, 1826 cm^{-1})[22a] **7a** appears to be a far stronger N donor. Of note is that the CO stretches for κ^2-complex **11** are weaker than those of κ^1-complex **10**, which illustrates that the additional coordination of the strong N donor provides a more electron-rich metal center with stronger W→(CO) backdonation. Single crystals of **10** were obtained by cooling a toluene solution. The molecular structure (Figure 9) shows a tight bond of the metal center with the *trans*-CO [W1–C19 = 2.0058(18) Å; W–C_{avg} = 2.046 Å] and a slightly weakened CO triple bond [C19–O1 = 1.142(2) Å; C–O_{avg} = 1.139 Å]. The W1–P1 distance [2.5333(4) Å] is comparable to the one in analogous PPh_3 and Ph_2PPy complexes.[22a,23] Further parameters of the ligand are similar to those for **6a**.

The influence of P substituents[5c] was apparent in [(**7**)$Rh^{III}(Cp^*)Cl_2$] complexes, which can equilibrate between P-κ^1 and P,N-κ^2 forms with characteristic ^{31}P NMR chemical shifts and coupling constants, as has been shown for related iminophosphanes (generally: $^1J_{P,Rh}{}^{\kappa1} \approx 146$ Hz; $^1J_{P,Rh}{}^{\kappa2} \approx 114$ Hz; for example [(Me-NC(Ph)P(3-Me-Ph)$_2$)RhCp*Cl$_2$] (P-κ^1: δ 34.7 ppm, $^1J_{P,Rh}$ = 144.6 Hz; P,N-κ^2: (δ −12.1 ppm, $^1J_{P,Rh}$ = 114.7 Hz); see also Figure 2).[6b,d] To obtain the complexes, **7** was reacted with

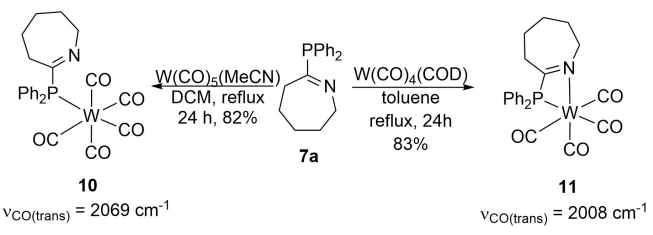

Scheme 5. Analysis of the donor capacity of **7a** by using $W(CO)_n$ complexes.

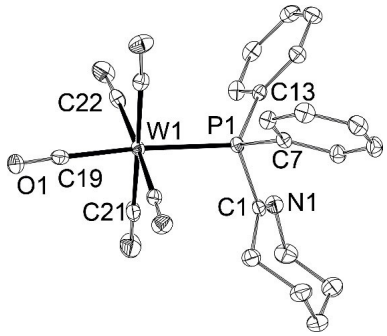

Figure 9. Displacement ellipsoid plot of the W carbonyl complex **10** at the 50% probability level. Hydrogen atoms are omitted for clarity. Selected bond lengths [Å] and angles [°]: W1–P1 = 2.5333(4), W1–C19 = 2.0058(18), C19–O1 = 1.142(2), P1–C13 = 1.8216(15), P1–C7 = 1.8234(16), P1–C1 = 1.8617(16), C1–N1 = 1.265(2), C19–W1–P1 = 175.60(5), O1–C19–W1 = 177.95(15), N1–C1–P1 = 117.22(12), C1–P1–W1–C21 = −15.71(8), C13–P1–W1–C22 = 14.32(7).

0.5 equiv. $[Rh^{III}Cp^*Cl_2]_2$ in CH_2Cl_2 (Scheme 6) to give exclusively P-κ^1 complexes for the *n*-butyl-substituted ligand (^{31}P NMR: **12b**: δ 29.7 ppm, $^1J_{P,Rh}$ = 134.2 Hz, major (98%); 21.3 ppm, $^1J_{P,Rh}$ = 136.2 Hz, minor (2%)) and mainly the P,N-κ^2 complex for the dicyclohexyl ligand (**12c**: δ −1.5 ppm, $^1J_{P,Rh}$ = 104.5 Hz, major (66%); 41.0 ppm, $^1J_{P,Rh}$ = 133.4 Hz, minor (18%); 31.2 ppm, $^1J_{P,Rh}$ = 130.6 Hz, minor (16%)). The observation of two P-κ^1 resonances suggests the presence of flippamers or rotamers; the absence of ^{31}P,^{31}P couplings rules out bridged complexes (μ coordination).

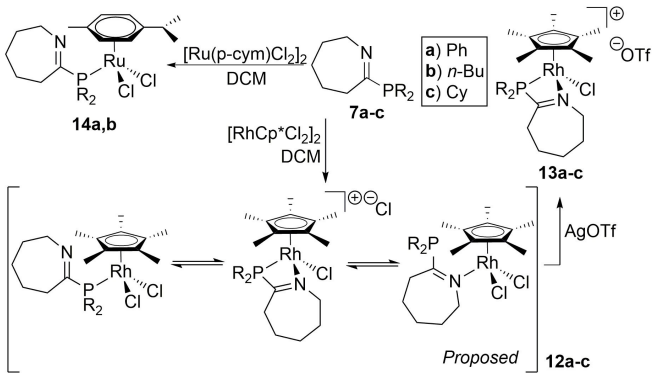

Scheme 6. The coordination of ligands **7** to Rh^{III} and Ru^{II}.

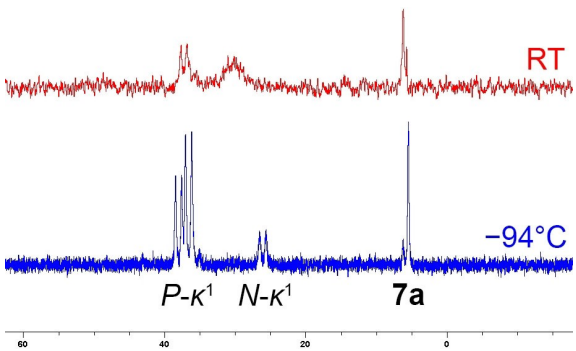

Figure 10. ^{31}P NMR spectra at room temperature and at −94 °C for complex **12a**.

Surprisingly, Rh complexation of phenyl ligand **7a** did not give a clean P-κ^1/κ^2 mixture. The ^{31}P NMR spectrum of complex **12a** showed a mixture of two broad signals (δ 36.9 ppm, d, $^1J_{P,Rh}$ = 142.5 Hz, (42%); δ 30.1 ppm, br s, (58%)) that resolved into three doublets on lowering the temperature to −94 °C (Figure 10). Their coupling constants suggests a mixture of two P-κ^1complexes (δ 38.0 ppm, $^1J_{P,Rh}$ = 139.3 Hz (31%); δ 36.5 ppm, $^1J_{P,Rh}$ = 137.7 Hz (54%)) and possibly an N-κ^1 complex, as it has a strikingly different P–Rh coupling and other coordination modes are unlikely due to the lack of additional P and/or Rh couplings. (δ 27.5 ppm, $J_{P,Rh}$ = 153.9 Hz (15%)). The N-monodentate coordination mode of 1,3-P,N ligands has been reported only for Mn^{II} and Fe^{II},[3,24] and not for rhodium. Apparently, the two P-κ^1 and one N-κ^1 bonding modes interchange rapidly at room temperature.

The competing P-κ^1/N-κ1 coordination modes for **12a** can be attributed to the C,N-dialkyl-P-phenyl substitution pattern of ligand **7a**. Its aryl groups reduce the donating property of the phosphane group as compared to **7b** and **7c**, and the cyclic alkyl chain makes its imine a stronger donor than in reported iminophosphanes.[6]

For comparison, we synthesized the Rh complexes of noncyclic ligand **9** (Scheme 4), which is similarly substituted as **7a**. The low temperature ^{31}P NMR spectrum showed the P-κ^1 complex (δ 39.1 ppm, $^1J_{P,Rh}$ = 144.2 Hz (55%); δ 27.7 ppm, $^1J_{P,Rh}$ = 132.8 Hz (29%)) together with small amounts of both the N-κ^1 complex (δ 33.9 ppm, $^1J_{P,Rh}$ = 152.3 Hz (4%)) and the P,N-κ^2 complex (δ −15.0 ppm, $^1J_{P,Rh}$ = 115.0 Hz (6%)) before AgOTf converted it fully to the κ^2 complex (72% yield, $\delta(^{31}P)$ −15.5 (d, $^1J_{P,Rh}$ = 114.6 Hz). Even though the amount of observed N-coordination is lower for **9** than for **7a**, these results highlight the influence of the C,N,P substituents of **7** on the P,N coordination mode.

All Rh-complexes **12a–c** could be fully converted to the bidentate complex **13** upon chloride abstraction with AgOTf (Scheme 6; **13a**: 82% yield, $\delta(^{31}P)$ −16.8 ppm, $^1J_{P,Rh}$ = 113.9 Hz; **13b**: 83% yield, $\delta(^{31}P)$ −19.7 ppm, $^1J_{P,Rh}$ = 110.0 Hz; **13c**: 76% yield, $\delta(^{31}P)$ −2.6 ppm, $^1J_{P,Rh}$ = 106.8 Hz).

Next, we explored the coordination to Ru^{II} (Scheme 6) and the catalytic activity[4a] of the resulting complexes. Reacting **7a,b** with $[Ru(p\text{-cym})Cl_2]_2$ (*p*-cym = *p*-cymene) provided the *P*-κ^1 complex **14b** (66%, $\delta(^{31}P)$ 27.3 ppm). Complex **14a** could not be isolated from the reaction mixture that showed the presence of two products ($\delta(^{31}P)$ 31.2 (27%), 23.4 (73%) ppm), which we tentatively assign to the *N*-κ^1 and *P*-κ^1 complexes, respectively, in analogy to Rh^{III} complex **12a** (see above).

Next, three Ru^{II} complexes of ligands **7a–c** were preliminarily tested for their effectiveness as catalysts in the solvent-free, closed-vessel hydration of benzonitrile[25] at 180 °C for 3 h (Table 2). Surprisingly, **14a** generated in situ with the phenyl substituted ligand **7a** proved to be quite an active catalyst, yielding 79% product. In situ generated **14b** with the *n*-butyl substituted ligand **7b** afforded a somewhat lower yield of 59%, which could be enhanced to 70% by preforming the catalyst

Table 2. Solvent-free catalyzed hydration of benzonitrile with precatalyst $[Ru(p\text{-}cym)Cl_2]$.[a]

	Ligand (L)	*T* [°C]	*t* [h]	Yield[b] [%]
1	**7a**	180	3	79
2	**7b**	180	3	59
3	**7b**[c]	180	3	70
4	**7c**	180	3	15
5	$PyPPh_2$	180	3	*6*[6d]

[a] Reaction conditions: Ph–C≡N (3.6 mmol), H_2O (7.2 mmol), 1.4 mol% $[Ru(p\text{-cym})Cl_2]$ and ligand **7**. [b] Determined by GC. [c] Preformed catalyst (**14b**).

(entries 2 and 3, respectively). The least effective catalyst was the Ru^{II} complex of ligand **7c**, giving a hydration yield of only 15% that may have its origin in the more limiting steric factors. Even though the catalytic conditions were not optimized in this brief screen, it is rewarding that a hydration yield as high as 79% was obtained for P-κ^1-Ru^{II} complex **14a**, which resembles the highest yield of 82% found for the comparable Ru catalyst with an acyclic iminophosphane.[25] Both perform much better than the analogous Ru complex of the established Ph_2PPy ligand, which gives a hydration yield of 6%.[6d]

As complex **14b** performed only modestly in the hydration of benzonitrile, we chose to further screen its potential by preliminarily exploring the transfer hydrogenation of cyclohexanone in *i*PrOH, under conditions adapted from Jalón et al., who used the analogous complex of 2-PPh_2-1-methylimidazole to obtain a hydrogenation yield of 21% on using a KOH/catalyst ratio of 333:1 and a substrate/catalyst ratio of 2000:1.[26,27] Table 3 summarizes the effect of changes in catalyst loading, reaction time, and the addition of KOH. After in situ generation of the catalyst, at 3 mol% catalyst loading the conversions were slow (up to 20 h; entries 1–3), but similar to the catalyst of Jalón et al.,[26] the catalyst was substantially more active in presence of KOH (entries 4 and 5). Even the corresponding κ^2-complex of **14b**, obtained by ion exchange with $NaBF_4$, was active under these conditions (entry 7). With 0.5 mol% catalyst and 2.5 mol% KOH, a reaction time of 2 h still resulted in the quantitative hydrogenation of cyclohexanone (entry 8). Last, as iridium(I) complexes are generally very active hydrogenation catalysts,[28] we also explored the in situ generation of [(**7b**)Ir(COD)Cl], which showed a similar trend as the Ru^{II} complexes (entries 9–11).

These preliminary screenings demonstrate that the conveniently in situ generated κ^1 and κ^2 complexes of Ru^{II} and Ir^{I} with cyclic 1,3-P,N ligand **7** are active catalysts that warrant further scrutiny.

Chirality

As, to the best of our knowledge, no asymmetric 1,3-P,N-ligand-based catalysts have been reported,[4] the synthesis of such ligands may be valuable. With a synthetic route toward cyclic iminophosphanes at hand, we pursued substituting the backbone with a chiral group by using an inexpensive terpenoid as asymmetric starting point. The readily available terpenoid L-menthone[12] is well-suited for this purpose, since its sizeable (2*S*)-*i*Pr group is expected to be favorable for asymmetric induction.[29] Following the synthesis of the chiral ligands, we report their Ru and Rh complexes and briefly reflect on their catalytic potential.

The asymmetric derivatives of **7** were pursued in analogy to the parent compound, albeit that the solventless oxime synthesis was not effective, but reacting L-menthone with the hydroxylamine·HCl salt in an EtOH/H_2O mixture did provide oxime **16** as a colorless liquid after purification by crystallization at 5 °C (73%; Scheme 7).[30] Subsequent treatment with MsCl, NEt_3 and benzotriazole induced the Beckmann rearrangement via **17** to the desired benzotriazolyl azepine adduct **19**, which was isolated as an orange liquid (90%).

Whereas the ring expansion could have generated either or both regioisomers **18** and **19** (Scheme 7, pathways **A** and **B**), the NMR spectra showed only a single set of signals for the Me and *i*Pr CH_3 groups ($\delta(^1H)$ 1.11, 1.08, 1.06 ppm; $\delta(^{13}C)$ 24.2, 20.1, 17.7 ppm), indicating the formation of a single isomer. Based on the reported selectivity of related asymmetric cyclohexanone substrates In the Beckmann rearrangement,[31] we expected the formation of **19** to be favored. Whereas crystals of **19**, grown in a MeCN solution at −20 °C, were too temperature sensitive to isolate for X-ray crystallography, protonation with HOTf in $CHCl_3$ gave a thermally stable salt (**20**, 79%) in sharp contrast to the highly unstable unsubstituted azepinium triflate **5**. Crystals

Table 3. Catalytic transfer hydrogenation of cyclohexanone.

	Precatalyst [M]	L	Cat. Loading [mol%]	*t* [h]	Yield[a] [%]	Additives
1	$[Ru(p\text{-cym})Cl_2]_2$	**7b**	3	2	3	–
2	$[Ru(p\text{-cym})Cl_2]_2$	**7b**	3	3	20	–
3	$[Ru(p\text{-cym})Cl_2]_2$	**7b**	3	20	quant.	–
4	$[Ru(p\text{-cym})Cl_2]_2$	**7b**	1	20	0	–
5	$[Ru(p\text{-cym})Cl_2]_2$	**7b**	1	4	quant.	5 mol% KOH
6	$[Ru(p\text{-cym})Cl_2]_2$	**7b**	1	4	0	1 mol% $NaBF_4$
7	$[Ru(p\text{-cym})Cl_2]_2$	**7b**	1	4	quant.	5 mol% KOH, 1 mol% $NaBF_4$
8	$[Ru(p\text{-cym})Cl_2]_2$	**7b**	0.5	2	quant.	2.5 mol% KOH
9	$[Ir(COD)Cl]_2$	**7b**	1	4	2	–
10	$[Ir(COD)Cl]_2$	**7b**	1	4	quant.	5 mol% KOH
11	$[Ir(COD)Cl]_2$	**7b**	1	4	84	5 mol% KOH, 1 mol% $NaBF_4$

Reaction conditions: cyclohexanone in *i*-PrOH (2 M), reflux. [a] Determined by GC.

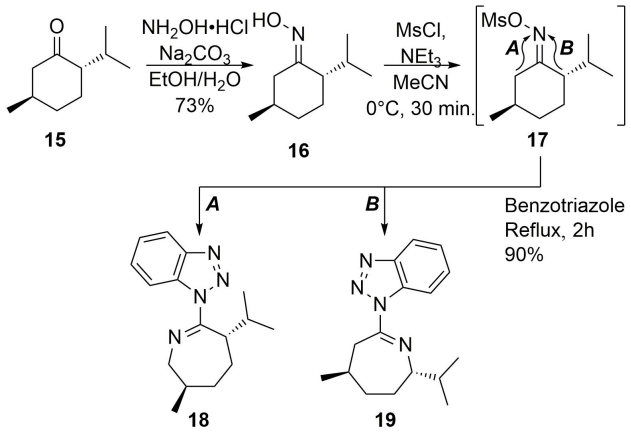

Scheme 7. Chiral benzotriazolyl-tetrahydroazepine synthesis.

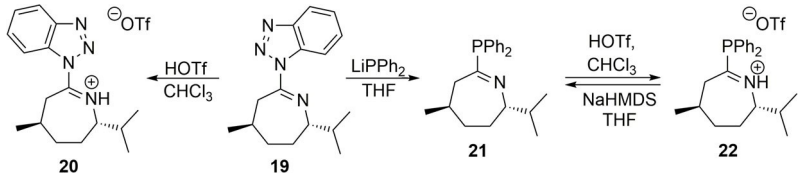

Scheme 8. Access to asymmetric ligands **21** from chiral benzotriazolyltetrahydroazepine **19**.

suitable for X-ray analysis were obtained by slow diffusion of pentane into a CH_2Cl_2 solution of **20**. Its molecular structure (Figure 11) concurs with the anticipated (2*S*,5*R*)-2-*i*Pr-5-Me regioisomer **19** with both alkyl groups in equatorial positions. Compared to the non-protonated **4** (Figure 6), the benzotriazolyl group of **20** is rotated by 155° and tilted with respect to the imine group [**20**: N1–C1–N2–N3 = −25.9(3); **4**: N1–C1–N2–N3 = 179.54(8)]. Clearly, protonation of the imine group prevents the intramolecular H-bonding that facilitated the planar conformation of **4**; the N1–H1 hydrogen interacts only with the triflate anion [H1···O1 = 1.97 (2) Å]. The positively charged N1 assumedly causes the slightly tighter benzotriazolyl bonding [**20**: C1–N2 = 1.384(3), N2–N3 = 1.403(3) Å; **4**: C1–N2 = 1.4334(12), N2–N3 = 1.3746(11) Å]. The parameters of the iminium group [C1–N1 = 1.280(3) Å, N1–C1–C6 = 122.68(19)°, C1–N1–C2 = 125.01(19)°] are comparable to those for **6a** and **6c** (Figure 6).

The introduction of the phosphane group on the chiral ring could not be achieved in analogy with the synthesis of the non-chiral ligands **7** (Scheme 3): surprisingly, treatment of the protonated precursor **20** with diphenylphosphane yielded its dehydrocoupling product tetraphenyldiphosphane.[32–34] Instead, the phosphane group was introduced by treating **19** with lithium phosphides $LiPR_2$ (R = Ph, *n*Bu) in THF to give the desired chiral cycloiminophosphane **21** in 53%, after purification by an acid/base work-up involving salt **22** (Scheme 8). The ^{31}P NMR spectrum showed a single resonance at δ 6.6, thus indicating the absence of flippamers, which was attributed to the reduced flexibility of the ring on which the *i*Pr and Me substituents favor equatorial positions.

Single crystals of **22** suitable for an X-ray structure determination were obtained by slow diffusion of pentane into a saturated CH_2Cl_2 solution. The molecular structure (Figure 12) shows a tetrahydroazepine chair similar to the one in **20** with the (2*S*)-*i*Pr and (5*R*)-Me indeed in equatorial positions and confirms that the stereochemical information of the L-menthone is retained over the synthesis. The conformation and bonding parameters of **22** compare closely to that of the achiral, unsubstituted **6a** (Figure 7) [**22**: C1–N1 = 1.289(2) Å,

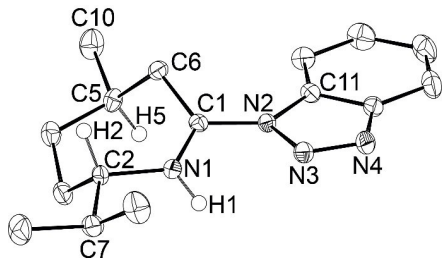

Figure 11. Displacement ellipsoid plot of 1-benzotriazolyl-(2*S*,5*R*)-2-isopropyl-5-methyl tetrahydroazepinium triflate **20** at the 50% probability level. The triflate anion and C–H hydrogen atoms are omitted for clarity, with exception of H2 and H5. Selected bond lengths [Å] and angles [°]: C1–N1 = 1.280(3), C1–N2 = 1.384(3), N1–C2 = 1.487(3), N1–H1 = 0.89(2), C1–C6 = 1.490(3), N2–N3 = 1.403(3), N3–N4 = 1.278(3), N2–C11 = 1.390(3), N1–C1–N2 = 117.2(2), N1–C1–C6 = 122.68(19), N2–C1–C6 = 120.1(2), C1–N1–C2 = 125.01(19), N1–C1–N2–N3 = −25.9(3), C6–C1–N2–N3 = 153.6(2).

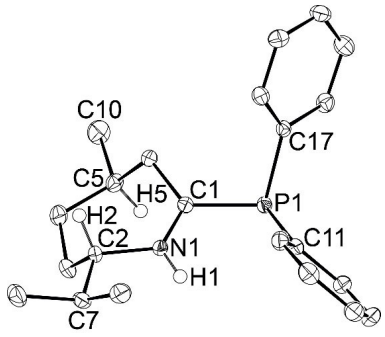

Figure 12. Displacement ellipsoid plot of (2*S*,5*R*)-phosphaazepinium triflate **22** at the 50% probability level. The triflate anion and C–H hydrogen atoms are omitted for clarity, with exception of H2 and H5. Selected bond lengths [Å] and angles [°]: P1–C1 = 1.8252(18), P1–C11 = 1.8217(19), P1–C17 = 1.8259(18), C1–N1 = 1.289(2), N1–C2 = 1.490(2), N1–C1–P1 = 121.79(14), N1–C1–C6 = 120.82 (16), C1–N1–C2 = 124.57(16).

P1–C1 = 1.8252(18) Å, N1–C1–P1 = 121.79(14)°; **6a**: N1–C1 = 1.2858(16) Å, P1–C1 = 1.8269(13) Å, N1–C1–P1 = 123.06(10)°].

Coordination of chiral ligand **21** to Ru^{II} gave the corresponding P-κ^1 complexes **23** (Scheme 9; 19%, $\delta(^{31}P)$ 24.8 ppm). Likewise, coordination of **21** to Rh^{III} afforded κ^1-Rh^{III} complex **24** that showed, akin to complex **12a** (see above), a broad ^{31}P NMR signal at room temperature, which resolved at −90 °C into a series of doublets with two major P-κ^1 resonances (δ 34.3 ppm, $^1J_{P,Rh}$ = 140.9 Hz, 38%; δ 22.8 ppm, $^1J_{P,Rh}$ = 142.5 Hz, 42%; Figure 13) and four minor ones with couplings indicative of P-κ^1 and κ^2 bonding (δ 29.9 ppm, $^1J_{P,Rh}$ = 140.9 Hz, 7%; δ 26.5 ppm, $^1J_{P,Rh}$ = 137.7 Hz, 7%; δ 24.7 ppm, $^1J_{P,Rh}$ = 137.7 Hz, 4%; δ 20.7 ppm, $^1J_{P,Rh}$ = 115.0 Hz, 2%). The P-κ^1 signals likely reflect different rotamers, as the absence of ^{31}P,^{31}P couplings rules out μ-complexation. In contrast to **12a**, no N-κ^1 signal was detected for **24**, presumably because the adjacent *i*Pr group discourages coordination at this site. Chloride abstraction converted **24** and its isomers to κ^2-**25** ($\delta(^{31}P, CH_2Cl_2)$ −11.3 ppm, $^1J_{P,Rh}$ = 106.6 Hz), which was calculated to be energetically favored by 3.1 kcal mol^{-1} over its epimer **25*** (ωB97XD/6-31 + G(d,p), Def2-TZVP for Rh).[6b,d,35–39] The obtained chiral transition metal complexes might be useful for asymmetric catalytic reactions, but such investigations were outside the scope of the present study. Based on the performance of ligands **7** (see above), asymmetric transfer hydrogenation seems a promising starting point.

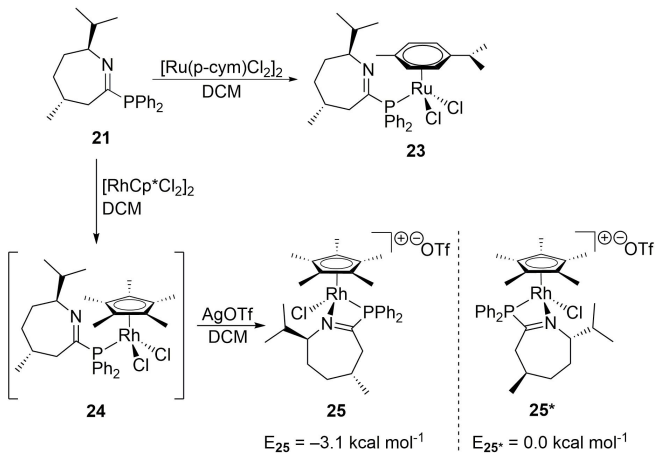

Scheme 9. The coordination of ligand **21** to Ru^{II} and Rh^{III}.

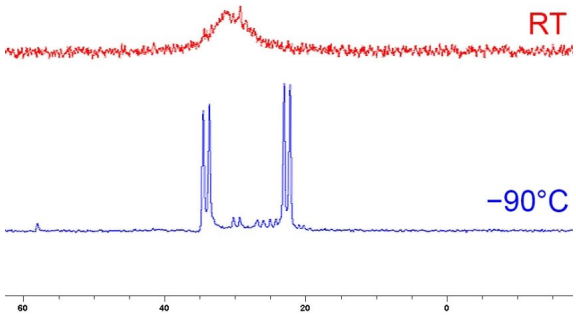

Figure 13. ^{31}P NMR spectra of **24** at room temperature and −90 °C.

Conclusion

This study reports the synthesis of cyclic 2-phospha-tetrahydroazepines as novel 1,3-P,N ligands with the intent of opening new opportunities in coordination chemistry and catalysis. This class of cycloiminophosphanes contains a seven-membered aliphatic imine ring with which it complements other classes of 1,3-P,N ligands, including the aromatic 2-pyridyl- and 2-imidazolyl-phosphanes, as well as the recently reported acyclic iminophosphanes and phosphaamidines. The ligands were readily obtained in a one-pot process through a Beckmann rearrangement of cyclohexanones to reactive nitrilium ion intermediates, which were trapped with benzotriazole. The benzotriazole was then quantitatively replaced with a secondary phosphane (R = Ph, *n*Bu, Cy), facilitated by triflic acid activation. With respect to other 1,3,-P,N ligands, these cycloiminophosphanes distinguish themselves by their high N-basicity and their flexible backbone, as ^{31}P NMR spectroscopy of the neutral ligands reveals the presence of flippamers, indicative of dynamic conformational behavior of the tetrahydroazepine ring. The ligands coordinate in both a P-κ^1 and a P,N-κ^2 fashion to W(carbonyl) complexes, which were analyzed by IR spectroscopy to quantify the ligands' donor strength. Coordination to $[RhCp^*Cl_2]_2$ gave a dynamic mixture of κ^1 and κ^2 complexes that, on treatment with silver triflate, lead only to the κ^2 complexes. Treatment with $[Ru(p\text{-cym})Cl_2]_2$ selectively provides P-κ^1 complexes, which were also effective catalysts for the hydration of benzonitrile (1.4 mol%, 180 °C, 3 h, up to 79%) and the transfer hydrogenation of cyclohexanone (0.5 mol%, 83 °C, 2 h, quant.); for the latter reaction iridium(I) could also be used (1 mol%, 83 °C, 4 h, quant.). Finally, as a preamble to asymmetric catalysis, a chiral cycloiminophosphane could be accessed from the natural precursor L-menthone in a selective Beckmann rearrangement. It was characterized by X-ray crystallography, and used to access Rh^{III} and Ru^{II} complexes. These chiral ligands form promising candidates for the future study of asymmetric 1,3-P,N catalysis.

Experimental Section

Preparation of compounds: The syntheses and full characterization of **4**–**7**, **9**–**14**, **19**–**25**, the Lewis acid catalyst screening of **4**, and the *P*-κ^1 and κ^2 Rh^{III} complexes of **9** are described in full detail (14 pages) in the Supporting Information, which also contains their ^1H, $^{13}C\{^1H\}$, $^{19}F\{^1H\}$, and ^{31}P NMR spectra (37 pages).

Computational procedure: Density functional calculations were performed at the ωB97X-D[36] level of theory using Gaussian09, revision A.02.[37] Geometry optimizations were performed using the 6-31 + G(d,p)[38] basis set (Def2-TZVP for Rh)[39] and the nature of each stationary point (see the Supporting Information) was confirmed by frequency calculations.

X-ray crystallography: Deposition Numbers 2084404 (for **4**), 2084405 (for **6a**), 2084406 (for **6c**), 2084407 (for **10**), 2084408 (for

20), and 2084409 (for **22**) contain the supplementary crystallographic data for this paper. These data are provided free of charge by the joint Cambridge Crystallographic Data Centre and Fachinformationszentrum Karlsruhe Access Structures service.

Acknowledgements

This work was supported by the Council for Chemical Sciences of The Netherlands Organization for Scientific Research (NWO/CW). We thank T. van Dijk for measuring high resolution mass-spectra and for fruitful discussions. M. K. Jongkind and R. Hoogendoorn are acknowledged for contributing to the synthesis of **9**. A. Chirila and M. M. Heeren contributed to screening suitable Beckmann rearrangement substrates.

Conflict of Interest

The authors declare no conflict of interest.

Keywords: cooperative effects · coordination modes · homogeneous catalysis · ligand design · N,P ligands

[1] For reviews on cooperative ligands, see: a) J. R. Khusnutdinova, D. Milstein, *Angew. Chem. Int. Ed.* **2015**, *54*, 12236-12273; *Angew. Chem.* **2015**, *127*, 12406–12445; b) J. I. van der Vlugt, *Eur. J. Inorg. Chem.* **2012**, 363–375.

[2] For a review on hybrid ligands, see: a) W.-H. Zhang, S. W. Chien, T. S. A. Hor, *Coord. Chem. Rev.* **2011**, *255*, 1991–2024; b) H. Grützmacher, *Angew. Chem. Int. Ed.* **2008**, *47*, 1814–1818; *Angew. Chem.* **2008**, *120*, 1838–1842; c) A. Bader, E. Lindner, *Coord. Chem. Rev.* **1991**, *108*, 27–110.

[3] For reviews on 2-pyridylphosphanes, see: a) G. R. Newkome, *Chem. Rev.* **1993**, *93*, 2067–2089; b) Z.-Z. Zhang, H. Cheng, *Coord. Chem. Rev.* **1996**, *147*, 1–39; c) P. Espinet, K. Soulantica, *Coord. Chem. Rev.* **1999**, *193-195*, 499–556.

[4] For reviews on 1,3-P,N ligated complexes, see: a) M. K. Rong, F. Holtrop, J. C. Slootweg, K. Lammertsma, *Coord. Chem. Rev.* **2019**, *380*, 1–16; b) M. K. Rong, F. Holtrop, J. C. Slootweg, K. Lammertsma, *Coord. Chem. Rev.* **2019**, *382*, 57–68; c) S. Maggini, *Coord. Chem. Rev.* **2009**, *253*, 1793–1832.

[5] 1,3-P,N ligand substituents affect κ^1/κ^2 coordination, see, for instance: a) L. Hintermann, T. T. Dang, A. Labonne, T. Kribber, L. Xiao, P. Naumov, *Chem. Eur. J.* **2009**, *15*, 7167–7179; b) P. C. Kunz, I. Thiel, A. L. Noffke, G. J. Reiß, F. Mohr, B. Spingler, *J. Organomet. Chem.* **2012**, *697*, 33–40; c) D. B. Grotjahn, Y. Gong, L. Zakharov, J. A. Golen, A. L. Rheingold, *J. Am. Chem. Soc.* **2006**, *128*, 438–453.

[6] a) T. van Dijk, S. Burck, M. K. Rong, A. J. Rosenthal, M. Nieger, J. C. Slootweg, K. Lammertsma, *Angew. Chem. Int. Ed.* **2014**, *53*, 9068-9071; *Angew. Chem.* **2014**, *126*, 9214–9217; b) T. van Dijk, S. Burck, A. J. Rosenthal, M. Nieger, A. W. Ehlers, J. C. Slootweg, K. Lammertsma, *Chem. Eur. J.* **2015**, *21*, 9328–9331; c) T. van Dijk, M. S. Bakker, F. Holtrop, M. Nieger, J. C. Slootweg, K. Lammertsma, *Org. Lett.* **2015**, *17*, 1461–1464; d) M. K. Rong, K. van Duin, T. van Dijk, J. J. M. De Pater, B.-J. Deelman, M. Nieger, A. W. Ehlers, J. C. Slootweg, K. Lammertsma, *Organometallics* **2017**, *36*, 1079–1090; e) T. van Dijk, M. K. Rong, J. E. Borger, M. Nieger, J. C. Slootweg, K. Lammertsma, *Organometallics* **2016**, *35*, 827–835.

[7] Also, see: a) X.-L. Chen, R. Yu, X.-Y. Wu, D. Liang, J.-H. Jia, C.-Z. Lu, *Chem. Commun.* **2016**, *52* 6288–6291; b) J. E. Radcliffe, A. S. Batsanov, D. M. Smith, J. A. Scott, P. W. Dyer, M. J. Hanton, *ACS Catal.* **2015**, *5*, 7095–7098; c) M. Fischer, H. Steinert, M. Schmidtmann, R. Beckhaus, *Dalton Trans.* **2019**, *48*, 1936–1940.

[8] For a review on nitrilium ion synthons, see: T. van Dijk, J. C. Slootweg, K. Lammertsma, *Org. Biomol. Chem.* **2017**, *15*, 10134–10144.

[9] "Caprolactam", J. Tinge, M. Groothaert, H. op het Veld, J. Ritz, H. Fuchs, H. Kieczka, W. C. Moran in *Ullmann's Encyclopedia of Industrial Chemistry*, Wiley-VCH, Weinheim, **2018**.

[10] See for instance: a) E. Beckmann, *Ber. Dtsch. Chem. Ges.* **1886**, *19*, 988; b) E. Beckmann, *Ber Dtsch. Chem. Ges.* **1887**, *20*, 1507; c) R. E. Gawley, *Organomet. React.* **1988**, *35*, 1–61; d) A. H. Blatt, *Chem. Rev.* **1933**, *12*, 215–260.

[11] a) A. R. Katritzky, C. Cai, S. K. J. Singh, *Org. Chem.* **2006**, *71*, 3375–3380; b) A. R. Katritzky, D. A. Monteux, D. O. Tymoshenko, *Org. Lett.* **1999**, *1*, 577–578; c) H. Pi, L. Liu, S. Jiang, W. Du, W. Deng, *Tetrahedron* **2010**, *66*, 6097–6100; d) A. R. Katritzky, X. Lan, J. Z. Yang, O. V. Denisko, *Chem. Rev.* **1998**, *98*, 409–548.

[12] E. Breitmaier, *Terpenes: Flavors, Fragrances, Pharmaca, Pheromones*, Wiley-VCH, Weinheim, **2006**.

[13] The success of ε-caprolactam conversion to its imidoyl halide varies between reports. See, for instance: a) G. Fodor, S. Nagubandi, *Tetrahedron* **1980**, *36*, 1279–1300; b) H. Bonnard, L. Ferrucio, J.-P. Senet, P.-Y. Le Roy, US6699988B2, **2004**; c) N. Nakajima, M. Ubukata, *Sci. Synth.* **2005**, *22*, 331–343; d) J. Jurczak, T. Koźluk, W. Kulicki, M. Pietraszkiewicz, J. Szymanski, *Synthesis* **1983**, *382*; e) Y. Ishida, S. Sasatani, K. Maruoka, H. Yamamoto, *Tetrahedron Lett.* **1983**, *24*, 3255–3258.

[14] Additional activation routes were explored in analogy to: a) A. B. Charette, S. Mathieu, J. Martel, *Org. Lett.* **2005**, *7*, 5401–5404; b) W. Z. Heldt, *J. Am. Chem. Soc.* **1958**, *80*, 5880–5885; c) Y. Matsumura, J. Fujiwara, K. Maruoka, H. Yamamoto, *J. Am. Chem. Soc.* **1983**, *105*, 6312–6314.

[15] I. Damljanovic, M. Vukicevic, R. D. Vukicevic, *Monatsh. Chem.* **2006**, *137*, 301–305.

[16] In situ generation of the sulfonate was preferable, since isolated batches of the mesylate, as well as its tosylate analogue, were highly reactive and prone to decomposition to thick black oils, suggestive of polymerization. See for instance: A. Kaneda, M. Nagatsuka, R. Sudo, *Bull. Chem. Soc. Jpn.* **1967**, *40*, 2705–2706.

[17] See for instance: F. Bertini, V. Lyaskovskyy, B. J. J. Timmer, F. J. J. de Kanter, M. Lutz, A. W. Ehlers, J. C. Slootweg, K. Lammertsma, *J. Am. Chem. Soc.* **2012**, *134*, 201–204.

[18] F. H. Allen, O. Kennard, D. G. Watson, *J. Chem. Soc. Perkin Trans. 2* **1987**, S1-S19.

[19] G. M. Chambers, R. Angamuthu, D. L. Gray, T. B. Rauchfuss, *Organometallics* **2013**, *32*, 6324–6329.

[20] a) B. L. Booth, K. O. Jibodu, M. F. Proença, *J. Chem. Soc. Chem. Commun.* **1980**, 1151–1153; b) B. L. Booth, K. O. Jibodu, M. F. J. R. P. Proença, *J. Chem. Soc. Perkin Trans. 1* **1983**, 1067–1073.

[21] See for instance: a) H. Oediger, F. Möller, K. Eiter, *Synthesis* **1972**, 591–598; b) F. Hibbert, K. P. P. Hunte, *J. Chem. Soc. Perkin Trans. 2* **1983**, 1895–1899; c) J. Tang, J. Dopke, J. G. Verkade, *J. Am. Chem. Soc.* **1993**, *115*, 5015–5020; d) Z. Glasovac, M. Eckert-Maksić, Z. B. Maksić, *New J. Chem.* **2009**, *33*, 588–597.

[22] a) K. Nishide, S. Ito, M. Yoshifuji, *J. Organomet. Chem.* **2003**, *682*, 79–84; b) J. Baur, H. Jacobsen, P. Burger, G. Artus, H. Berke, L. Dahlenburg, *Eur. J. Inorg. Chem.* **2000**, 1411–1422; c) R. J. Angelici, M. D. Malone, *Inorg. Chem.* **1967**, *6*, 1731–1736.

[23] A. G. Orpen, L. Brammer, F. H. Allen, O. Kennard, D. G. Watson, R. Taylor, *J. Chem. Soc. Dalton Trans.* **1989**, S1-S83.

[24] a) P. Braunstein, D. G. Kelly, A. Tiripicchio, F. Ugozzoli, *Bull. Soc. Chim. Fr.* **1995**, *132*, 1083–1086; b) E. C. Carson, S. J. Lippard, *J. Am. Chem. Soc.* **2004**, *126*, 3412–3413; c) E. S. Donovan, B. M. Barry, C. A. Larsen, M. N. Wirtz, W. E. Geiger, R. A. Kemp, *Chem. Commun.* **2016**, *52*, 1685–1688.

[25] a) R. García-Álvarez, S. E. García-Garrido, J. Díez, P. Crochet, V. Cadierno, *Eur. J. Inorg. Chem.* **2012**, 4218–4230; b) M. Muranaka, I. Hyodo, W. Okumura, T. Oshiki, *Catal. Today* **2011**, *164*, 552–555; c) T. Oshiki, H. Yamashita, K. Sawada, M. Utsunomiya, K. Takahashi, K. Takai, *Organometallics* **2005**, *24*, 6287–6290; d) R. García-Álvarez, J. Francos, E. Tomás-Mendivil, P. Crochet, V. Cadierno, *J. Organomet. Chem.* **2014**, *771*, 93–104; e) T. J. Ahmed, S. M. M. Knapp, D. R. Tyler, *Coord. Chem. Rev.* **2011**, *255*, 949–974.

[26] A. Caballero, F. A. Jalón, B. R. Manzano, G. Espino, M. Pérez-Manrique, A. Mucientes, F. J. Poblete, M. Maestro, *Organometallics* **2004**, *23*, 5694–5706.

[27] a) I. Moldes, E. de la Encarnación, J. Ros, Á. Alvarez-Larena, J. F. Piniella, *J. Organomet. Chem.* **1998**, *566*, 165–174; b) P. Kumar, A. Kumar Singh, M. Yadav, P.-Z. Li, S. Kumar Singh, Q. Xu, D. Shankar Pandey, *Inorg. Chim. Acta* **2011**, *368*, 124–131; c) P. Kumar, A. Kumar Singh, S. Sharma, D. Shankar Pandey, *J. Organomet. Chem.* **2009**, *694*, 3643–3652; d) M. Yamakawa, H. Ito, R. Noyori, *J. Am. Chem. Soc.* **2000**, *122*, 1466–1478.

[28] For a review on (asymmetric) Ir^{I}-catalyzed transfer hydrogenations, see: T. L. Church, P. G. Andersson, *Coord. Chem. Rev.* **2008**, *252*, 513–531.
[29] See for instance: T. Jerphagnon, J.-L. Renaud, C. Bruneau, *Tetrahedron: Asymmetry* **2004**, *15*, 2101–2111.
[30] J. Kulisch, M. Nieger, F. Strecker, A. Fischer, S. R. Waldvogel, *Angew. Chem. Int. Ed.* **2011**, *50*, 5564–5567; *Angew. Chem.* **2011**, *123*, 5678–5682.
[31] a) L. M. Fleury, E. E. Wilson, M. Vogt, T. J. Fan, A. G. Oliver, B. L. Ashfeld, *Angew. Chem. Int. Ed.* **2013**, *52*, 11589–11593; *Angew. Chem.* **2013**, *125*, 11803–11807; b) K. Hattori, Y. Matsumura, T. Miyazaki, K. Maruoka, H. Yamamoto, *J. Am. Chem. Soc.* **1981**, *103*, 7368–7370; c) K. Maruoka, T. Miyazaki, M. Ando, Y. Matsumura, S. Sakane, K. Hattori, H. Yamamoto, *J. Am. Chem. Soc.* **1983**, *105*, 2831–2843; d) N. Komatsu, S. Simizu, T. Sugita, *Syn. Comm.* **1992**, *22*, 277–279.
[32] The same reactivity was observed when the primary phosphane Mes*-PH_2 was used, which gave Mes*-PH-PH-Mes*. To the best of our knowledge, no similar organocoupling reagents have been reported to facilitate P–P bond formation.
[33] For more information on (main-group) catalyst mediated dehydrocouplings, see, for instance: a) R. J. Less, R. L. Melen, V. Naseri, D. S. Wright, *Chem. Commun.* **2009**, 4929–4937; b) R. L. Melen, *Chem. Soc. Rev.* **2016**, *45*, 775–788; c) R. J. Less, R. L. Melen, D. S. Wright, *RSC Adv.* **2012**, *2*, 2191–2199.
[34] For more information on diphosphanes, see for instance: a) C. N. Smit, Th. A. van der Knaap, F. Bickelhaupt, *Tetrahedron Lett.* **1983**, *24*, 2031–2034; b) C. M. D. Komen, F. J. J. de Kanter, S. J. Goede, F. Bickelhaupt, *J. Chem. Soc. Perkin Trans. 2* **1993**, 807–812.
[35] For similar epimerism in the κ^2-[RuCp*Cl] complexes of chiral 1,4-P,N ligands, see: M. Ito, A. Osaku, C. Kobayashi, A. Shiibashi, T. Ikariya, *Organometallics* **2009**, *28*, 390–393.
[36] a) J.-D. Chai, M. Head-Gordon, *Phys. Chem. Chem. Phys.* **2008**, *10*, 6615–6620; b) J.-D. Chai, M. Head-Gordon, *J. Chem. Phys.* **2008**, *128*, 084106.
[37] M. J. Frisch, G. W. Trucks, H. B. Schlegel, G. E. Scuseria, M. A. Robb, J. R. Cheeseman, G. Scalmani, V. Barone, B. Mennucci, G. A. Petersson, H. Nakatsuji, M. Caricato, X. Li, H. P. Hratchian, A. F. Izmaylov, J. Bloino, G. Zheng, J. L. Sonnenberg, M. Hada, M. Ehara, K. Toyota, R. Fukuda, J. Hasegawa, M. Ishida, T. Nakajima, Y. Honda, O. Kitao, H. Nakai, T. Vreven, J. A. Montgomery Jr., J. E. Peralta, F. Ogliaro, M. Bearpark, J. J. Heyd, E. Brothers, K. N. Kudin, V. N. Staroverov, R. Kobayashi, J. Normand, K. Raghavachari, A. Rendell, J. C. Burant, S. S. Iyengar, J. Tomasi, M. Cossi, N. Rega, J. M. Millam, M. Klene, J. E. Knox, J. B. Cross, V. Bakken, C. Adamo, J. Jaramillo, R. Gomperts, R. E. Stratmann, O. Yazyev, A. J. Austin, R. Cammi, C. Pomelli, J. W. Ochterski, R. L. Martin, K. Morokuma, V. G. Zakrzewski, G. A. Voth, P. Salvador, J. J. Dannenberg, S. Dapprich, A. D. Daniels, O. Farkas, J. B. Foresman, J. V. Ortiz, J. Cioslowski, D. J. Fox, *Gaussian 09, Revision A.02*; Gaussian, Inc., Wallingford, CT, **2009**.
[38] a) R. Ditchfield, W. J. Hehre, J. A. Pople, *J. Chem. Phys.* **1971**, *54*, 724–728; b) W. J. Hehre, R. Ditchfield, J. A. Pople, *J. Chem. Phys.* **1972**, *56*, 2257–2261; c) P. C. Hariharan, J. A. Pople, *Theor. Chem. Acc.* **1973**, *28*, 213–222; d) P. C. Hariharan, J. A. Pople, *Mol. Phys.* **1974**, *27*, 209–214; e) M. S. Gordon, *Chem. Phys. Lett.* **1980**, *76*, 163–168; f) M. M. Francl, W. J. Pietro, W. J. Hehre, J. S. Binkley, D. J. DeFrees, J. A. Pople, M. S. Gordon, *J. Chem. Phys.* **1982**, *77*, 3654–3665; g) R. C. Binning Jr., L. A. Curtiss, *J. Comb. Chem.* **1990**, *11*, 1206–1216; h) J.-P. Blaudeau, M. P. McGrath, L. A. Curtiss, L. Radom, *J. Chem. Phys.* **1997**, *107*, 5016–5021; i) V. A. Rassolov, J. A. Pople, M. A. Ratner, T. L. Windus, *J. Chem. Phys.* **1998**, *109*, 1223–1229; j) V. A. Rassolov, M. A. Ratner, J. A. Pople, P. C. Redfern, L. A. Curtiss, *J. Comb. Chem.* **2001**, *22*, 976–984; k) T. Clark, J. Chandrasekhar, G. W. Spitznagel, P. V. R. Schleyer, *J. Comb. Chem.* **1983**, *4*, 294–301.
[39] D. Andrae, U. Häußermann, M. Dolg, H. Stoll, H. Preuß, *Theor. Chim. Acta* **1990**, *77*, 123–141.

Manuscript received: June 1, 2021
Accepted manuscript online: August 17, 2021
Version of record online: September 8, 2021

